ACS OMEGA

Open Access

http://pubs.acs.org/journal/acsodf

Article

Constraint-Induced Movement Therapy Modulates Neuron Recruitment and Neurotransmission Homeostasis of the Contralesional Cortex to Enhance Function Recovery after Ischemic Stroke

Anjing Zhang,[†] Ying Xing,[†] Jiayuan Zheng, Congqin Li, Yan Hua, Jian Hu, Zhanzhuang Tian,* and Yulong Bai*

Cite This: *ACS Omega* 2024, 9, 21612−21625

Read Online

ACCESS | Metrics & More | Article Recommendations

ABSTRACT: Stroke often results in long-term and severe limb dysfunction for a majority of patients, significantly limiting their activities and social participation. Constraint-induced movement therapy (CIMT) is a rehabilitation approach aimed explicitly at enhancing upper limb motor function following a stroke. However, the precise mechanism remains unknown. This study explores how CIMT may alleviate forelimb paralysis in ischemic mice, potentially through structural and functional remodeling of brain regions beyond the infarct area, especially the contralateral cortex. We demonstrated that CIMT recruits neurons from the contralesional cortex into the network that innervates the affected forelimb, as evidenced by PRV retrograde nerve tracing. Additionally, we investigated how CIMT influences synaptic plasticity in the contralateral cortex by evaluating synaptic growth marker levels and neurotransmission's homeostatic regulation. Our findings uncover a rehabilitative mechanism by which CIMT treats ischemic stroke, characterized by increased recruitment of neurons from the contralateral cortex into the network that innervates the affected forelimb, facilitated by homeostatic regulation of neurotransmission.

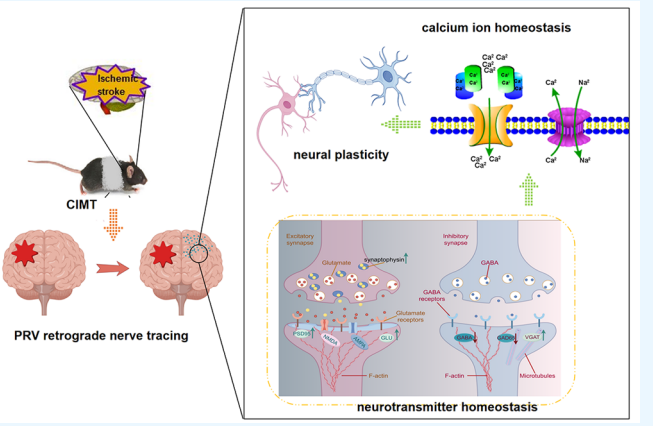

INTRODUCTION

Stroke is a common cerebrovascular disease characterized by high disability, morbidity, and mortality worldwide. The majority of stroke patients showed long-term and severe limb dysfunction, which limits their activities and social participation.[1,2] Therefore, exploring effective strategies that can facilitate the recovery of limb motor function after a stroke is very important. Constraint-induced movement therapy (CIMT) is a rehabilitation therapy designed to improve upper limb motor function after stroke.[3] In animal and clinical studies, CIMT is widely used to improve the affected limb function after stroke by forcing the use of the affected limb and restricting the use of the healthy side.[4,5] However, the mechanisms of CIMT are still unclear. It is necessary to explore the pathophysiological mechanism of rehabilitation therapy for a cerebral stroke.

Neural plasticity plays an essential role in neural development and recovery following brain ischemic injury, involving axonal sprouting, alterations in synaptic strength, formation of new synapses, compensation by the contralateral cortex, and so on.[6,7] Rehabilitative training can subserve synaptogenesis and increase the stability of those newborn synapses, such as physical exercise training and CIMT.[8−11] It has been reported that the exercise-induced paralysis recovery of brain ischemic rats may be related to the upregulation of both GAP-43 phosphorylated at serine 41 (pSer41-GAP-43) and GAP-43. The possible mechanisms, which include neurite formation, synaptic connections and remodeling, might be related to the interaction between GAP-43 and calmodulin, PKC, and nerve growth factor (NGF).[12] Thus, rehabilitation training might be an effective rehabilitative strategy to improve dysfunction by modulating neural plasticity.

Received: March 15, 2024
Revised: April 18, 2024
Accepted: April 24, 2024
Published: May 3, 2024

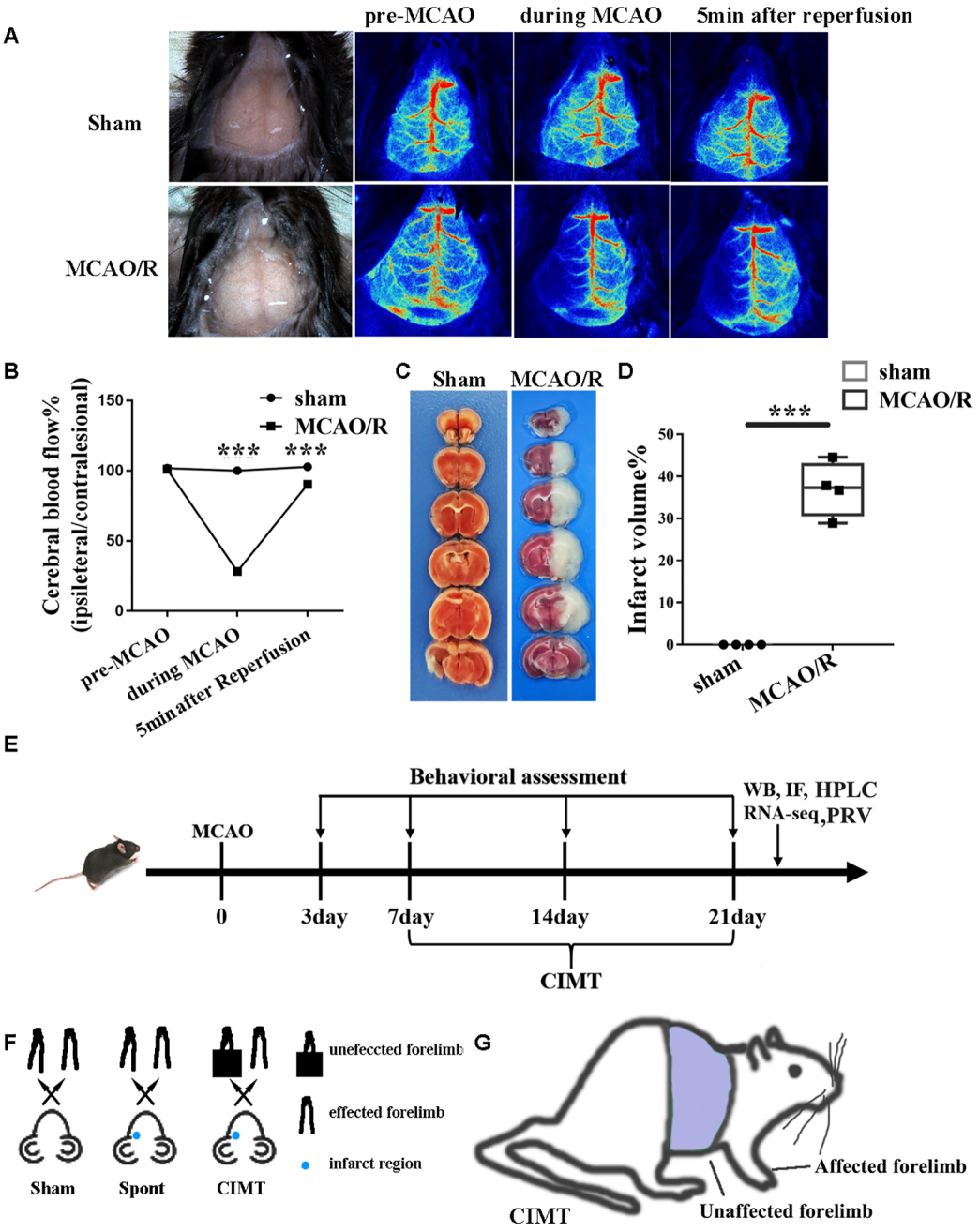

Figure 1. MCAO model establishment and CIMT intervention. (A) The rCBF% of Sham and MCAO/R mice was assessed by laser speckle imaging pre-MCAO, during MCAO and 5 min after reperfusion. (B) Quantitative analysis showing the rCBF% of Sham and MCAO/R mice. (C) TTC staining assessed the successful establishment of the MCAO model on the third day after surgery. (D) Quantitative analysis showing the infarct volume of Sham and MCAO/R mice; (E) Timeline of the experiments showed that CIMT was applied at postsurgery 7−21 days; (F, G) The experimental design in Sham, Spont, and CIMT group. Data are analyzed by one-way ANOVA followed by Bonferroni post hoc. Asterisks indicate significances: $*p < 0.05$, $**p < 0.01$, and $***p < 0.001$. CIMT: constraint-induced movement therapy, MCAO/R: middle cerebral artery occlusion/reperfusion, TTC: 2,3,5-triphenyltetrazolium chloride.

Structural and functional remodeling of regions beyond the infarct area can change activity within bilateral neuronal networks, which promotes functional recovery.[13] Clinical studies have found that the contralesional hemisphere also shows extensive activation when performing hemiplegic body movements, which is higher than that of healthy people performing the same movements.[14] Naohiko et al. showed that CIMT can effectively improve forelimb motor dysfunction caused by severe ischemia of the primary motor cortex (M1) by enhancing corticospinal projection from the surrounding infarct area.[15] In our previous study, CIMT can significantly improve the synapse number of the contralesional cortex and elicit more neuron recruitment into the paralyzed forelimb-innervating network from the contralesional hemisphere, such as the red nucleus.[16] However, the mechanism of the CIMT-regulated paralyzed forelimb-innervating network needs to be explored further.

https://doi.org/10.1021/acsomega.4c02537
ACS Omega 2024, 9, 21612−21625

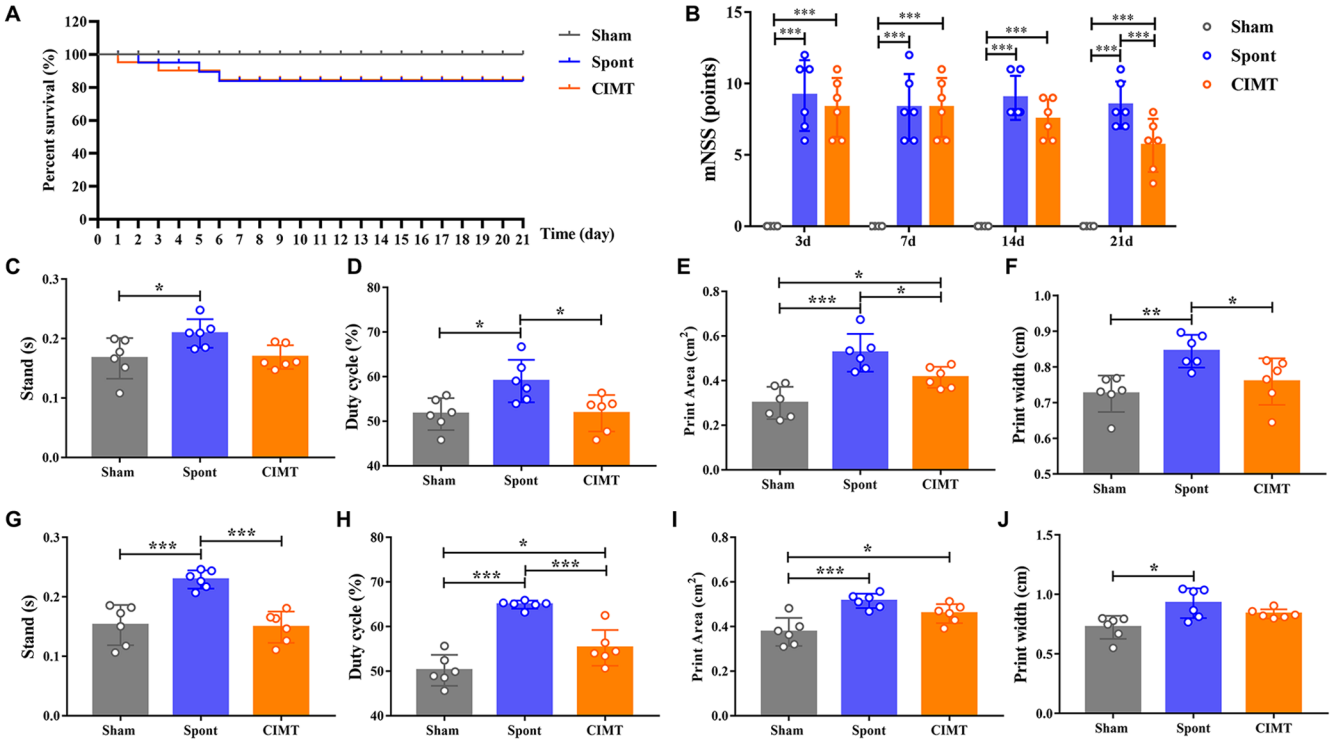

Figure 2. CIMT increased the recovery of motor function on the 21st day after ischemic stroke. (A) Survival curve in each group during 21 days after ischemic stroke. Data were assessed using survival analysis by the log-rank (Mantel-Cox) test. (B) mNSS score was performed on the 3rd, 7th, 14th, and 21st days after the stroke. (C−F) The stand, the duty cycle, the print area, and the print width of the affected forelimb were measured by a catwalk test. (G−J) The stand, the duty cycle, the print area, and the print width of the affected hindlimb were measured by using the catwalk test. Data are expressed as mean ± SD ($n = 6$). Data are analyzed by one-way ANOVA followed by Bonferroni post hoc. Asterisks indicate significances: *$p < 0.05$, **$p < 0.01$, and ***$p < 0.001$. mNSS: modified neurological severity score, CIMT: constraint-induced movement therapy.

In this study, we investigated the possible mechanisms of CIMT in improving forelimb paralysis in ischemic mice, which is involved in the CIMT-induced functional compensation of the contralesional cortex. We explored the CIMT-recruited neurons from the contralateral cortex into the affected forelimb-innervating network by pseudorabies virus (PRV) retrograde nerve tracing. We also study CIMT-facilitated changes in synaptic plasticity of the contralateral cortex by assessing the marker levels of synaptic growth and the homeostatic regulation of neurotransmission on the contralateral cortex. This study revealed a rehabilitative mechanism for CIMT treatment of ischemic stroke that involves the increased neuron recruitment from the contralateral cortex into the affected forelimb-innervating network by the homeostatic regulation of neurotransmission.

RESULTS

1. Successfully Established MCAO Models. The success of the MCAO model was verified by laser speckle imaging. The rCBF% were significantly decreased during MCAO and increased after reperfusion than those in the Sham mice ($p < 0.001$, Figure 1A, B). On the third day after MCAO/R, TTC staining showed a significant infarct area in the left hemisphere ($p < 0.001$, Figure 1C, D).

2. CIMT Improved Motor Function after Ischemic Stroke. Mice in the Sham group showed 100% survival during the 21 day observation period. There was no significant difference in survival between the Spont and CIMT groups ($p > 0.05$, Figure 2A). We used mNSS to assess the recovery of motor function after CIMT. In the Spont and CIMT group, the mNSS of mice was significantly increased compared to those in the Sham group on the third, seventh, 14th, and 21st day after stroke ($p < 0.001$). However, the mNSS were decreased in the CIMT group than those in the Spont group on the 21st day after stroke ($p < 0.001$, Figure 2B). Behavioral deficits following a stroke were also evaluated using catwalk tests. In the Spont group, significant increases were observed in the stand time, duty cycle, print area, and print width in the affected forelimb and hindlimb, compared to the Sham group. Conversely, the CIMT group displayed noticeable reductions in the duty cycle, print area, and print width of the affected forelimb, as well as the stand time and duty cycle of the affected hindlimb, compared to the Spont group. Additionally, aside from the print area of the affected forelimb as well as the duty cycle and the print area of the affected hindlimb in the CIMT group, which were still more significant than those in the Sham group ($p < 0.05$), no significant differences were observed in other indices between the two groups (Figure 2C−J). These results indicate a practical improvement in motor function in the affected forelimb and hindlimb following CIMT.

3. CIMT Recruited Neurons of the Contralesional Motor Cortex into the Innervating Network of the Affected Upper Limb. The PRV-positive cells can be colocalized with the NEUN-positive cells, indicating that the PRV transfected neurons (Figure 3A). PRV-positive neurons were counted in the primary motor cortex (M1) and primary somatosensory cortex (S1) in the ipsilesional and contrale-

https://doi.org/10.1021/acsomega.4c02537
ACS Omega 2024, 9, 21612−21625

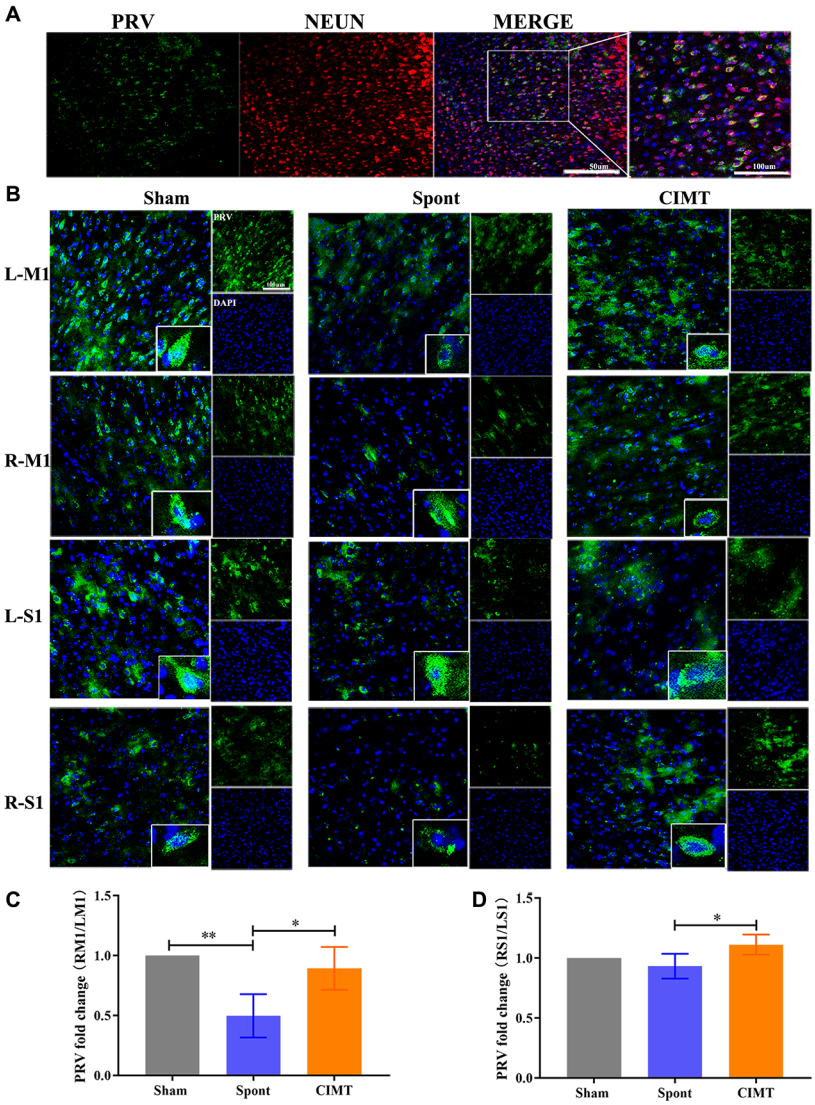

Figure 3. CIMT recruited neurons of the contralesional motor cortex into the innervating network of the affected upper limb. The pseudorabies virus (PRV) infection from the affected (right side) brachial plexus was used to identify the origin of central nervous system projections. (A) The colocalization of PRV and NEUN in the cortex of the Sham group; (B) The expression of PRV in the M1 and S1 areas both in the contralesional (R) and ipsilesional (L) hemispheres. (C, D) The statistical analysis of the number changes in PRV-positive cells among there groups (RM1/LM1, RS1/LS1). Data are expressed as the mean ± SD (n = 4−6). Data are analyzed by one-way ANOVA followed by Bonferroni post hoc. Asterisks indicate significances: *p < 0.05, **p < 0.01, and ***p < 0.001. CIMT: constraint-induced movement therapy, L: ipsilesional, R: contralesional, M1: primary motor cortex, S1: primary somatosensory cortex.

sional hemispheres. In Figure 3B, the radio of contralesional M1/ipsilesional M1 in the Spont group was lower than in the Sham and CIMT groups (p < 0.05). The radio of contralesional S1/ipsilesional S1 in the CIMT group was significantly higher compared to the Spont group (p < 0.05). No significant difference was observed between the Sham group and the CIMT group.

4. RNA-seq Showed the Potential Mechanism of CIMT-Reversed Motor Dysfunction. Transcriptome-wide RNA sequencing and bioinformatics analysis were performed to explore the potential mechanism of CIMT-reversed motor dysfunction. We found 559 differentially expressed genes (DEGs) between the Sham and Spont groups and 663 differentially expressed genes between the Spont and CIMT groups. Among those differentially expressed genes, 169 differentially expressed genes were found in the Sham, Spont, and CIMT groups (Figure 4A−D). We further analyzed the biological functions of the differentially expressed genes using GO annotation analysis and KEGG analysis. The natural process-related genes annotated with GO terms were involved in "cellular calcium ion homeostasis", "gamma-aminobutyric acid signaling pathway", "regulation of gamma-aminobutyric acid secretion", and "regulation of synaptic transmission, cholinergic", indicating the critical role of cellular calcium ion homeostasis in CIMT improving motor function (Figure 4E). The associated enriched pathway by KEGG enrichment analysis was involved in the "VEGF signaling pathway" and the "glutamatergic synapse" (Figure 4F).

5. CIMT facilitated the synaptic plasticity of the contralateral cortex after ischemic stroke. The expressions of synaptic associated proteins in the contralateral cortex were evaluated on the 21st day after ischemic stroke. Compared to the Sham and the Spont group, the expression of PSD95 and GAP43 in the contralateral cortex of the CIMT

https://doi.org/10.1021/acsomega.4c02537
ACS Omega 2024, 9, 21612−21625

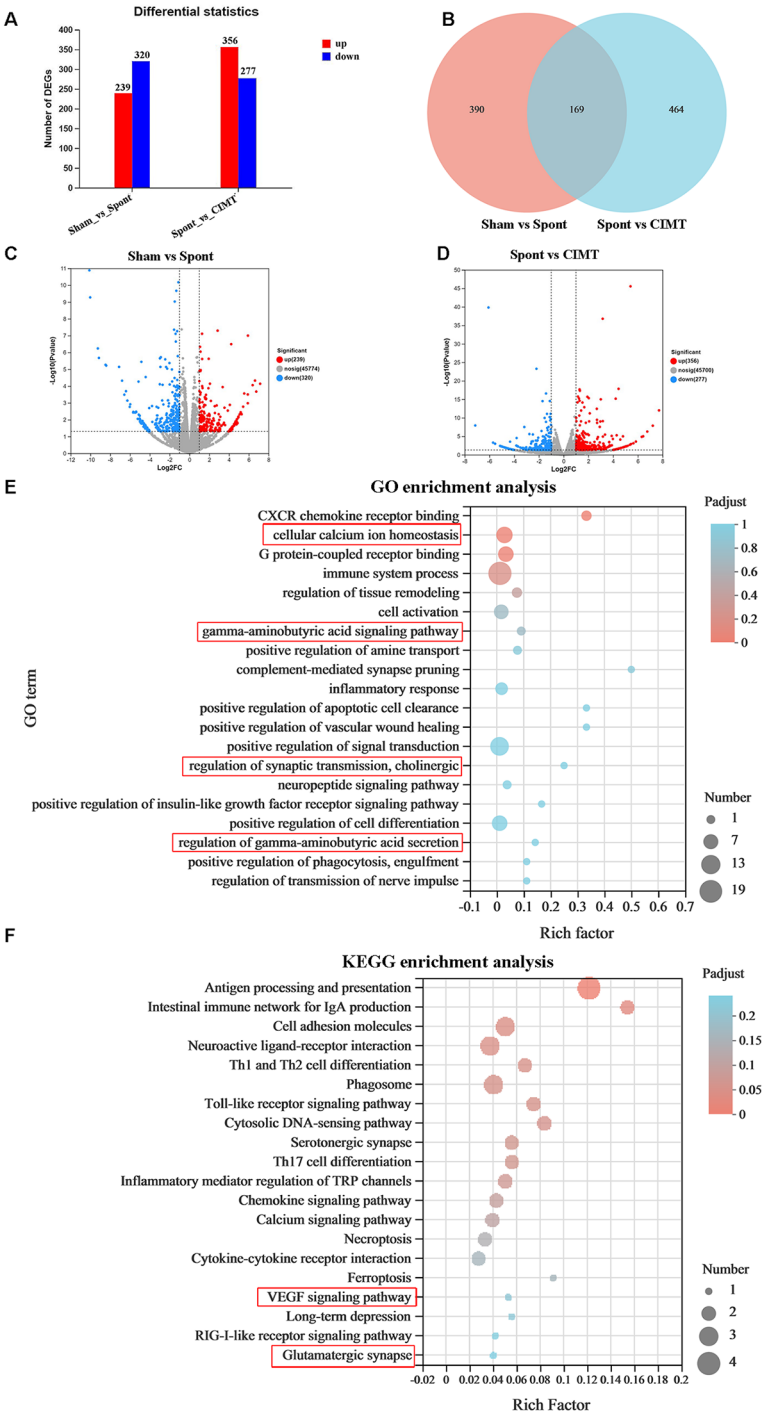

Figure 4. Changes in synaptic plasticity in the contralateral cortex of ischemic mice after CIMT. (A) Histogram of 559 DEGs with 239 upregulated genes and 320 downregulated genes between the Sham and Spont groups. Histogram of 633 DEGs with 356 up-regulated genes and 277 down-regulated genes between the CIMT and Spont groups. (B) There were 169 DEGs between Sham vs Spont groups and CIMT vs Spont groups. (C, D) Volcano plots of DEGs between the Sham vs Spont groups and CIMT vs Spont groups. Red dots: the significantly upregulated genes. Green dots: the significantly downregulated genes. Gray dots: the nonsignificant genes. (E) GO term enrichment analysis of DEGs revealed that CIMT facilitated motor recovery possibly by "cellular calcium ion homeostasis", "gamma-aminobutyric acid signaling pathway", "regulation of gamma-aminobutyric acid secretion", and "regulation of synaptic transmission, cholinergic". (F) KEGG enrichment analysis of DEGs revealed the associated pathways, such as the "VEGF signaling pathway" and "Glutamatergic synapse". Data are expressed as the mean ± SD (n = 3). CIMT: constraint-induced movement therapy. DEGs: differentially expressed genes.

group was significantly increased ($p < 0.05$). There was no apparent difference between the Sham and Spont groups (Figure 5A–D). The levels of SYN were obviously elevated in the CIMT group than those in the Sham group ($p < 0.05$). However, there was no significant difference in the SYN expression between the Spont and CIMT groups (Figure 5E, F). To further explore the mechanisms of CIMT in ischemic stroke, the expression of CREB was assessed in Sham mice,

https://doi.org/10.1021/acsomega.4c02537
ACS Omega 2024, 9, 21612−21625

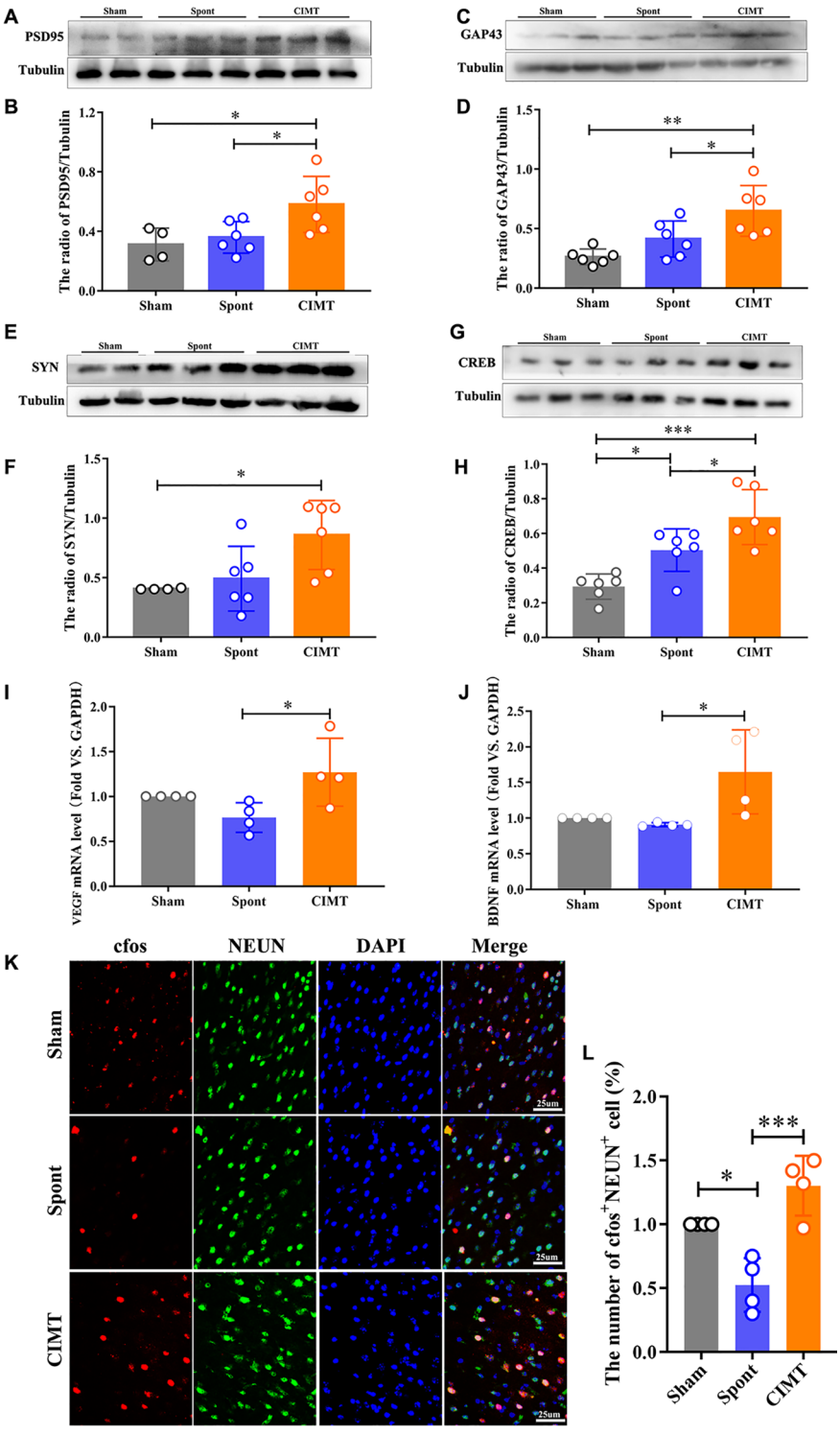

Figure 5. CIMT promoted expression of synaptic associated proteins after ischemic stroke. (A–L) A representative band and quantitative analysis show the expression of (A, B) PSD95, (C, D) GAP43, (E, F) SYN, and (G, H) CREB by Western blot. (I, J) The mRNA expression levels of (I) VEGF and (J) BDNF were quantified by PCR. Data are expressed as the mean ± SD (n = 4–6). (K) The expression of cfos in the contralesional cortex is assessed by IF. (L) Quantitative analysis showing the expression of cfos in the contralesional contralesional cortex. Data are analyzed by one-way ANOVA followed by Bonferroni post hoc. Asterisks indicate significances: *p < 0.05, **p < 0.01, and ***p < 0.001. CIMT: constraint-induced movement therapy, PSD-95: postsynaptic density 95, CREB: cAMP-response element binding protein, SYN: synaptophysin, VEGF: vascular endothelial growth factor, BDNF: brain-derived nerve growth factor.

CIMT mice, and Spont mice in the third week after MCAO surgery. In Figure 5G, H, the expression of CREB was found to be elevated in Spont mice (p < 0.05) and significantly higher in CIMT mice (p < 0.0001) compared to Sham mice. Additionally, the CIMT group exhibited a greater CREB expression increase than the Spont group (p < 0.05) (Figure

https://doi.org/10.1021/acsomega.4c02537
ACS Omega 2024, 9, 21612−21625

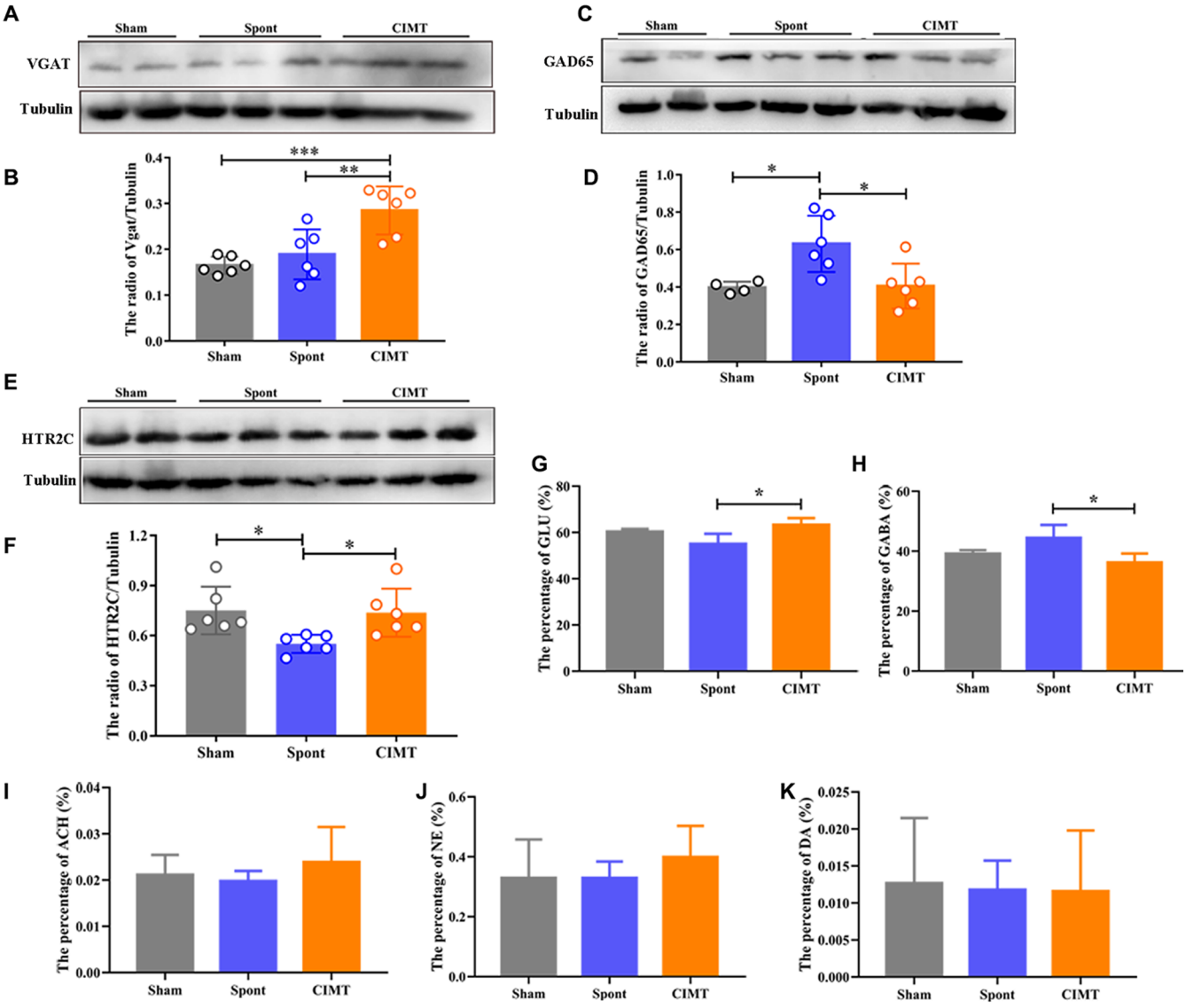

Figure 6. CIMT medicated the neurotransmitter homeostasis of the contralateral cortex. (A–F) A representative band and quantitative analysis showed the expression of (A, B) VGAT, (C, D) GAD65, and (E, F) HTR2C by Western blot. Data are expressed as the mean ± SD (n = 4–6). (G) Glutamate was significantly increased on the 21st day after ischemic stroke after CIMT. (H) GABA was significantly reduced on the 21st day after ischemic stroke after CIMT. (I–K) The levels of ACH, NE and DA showed no significant difference. Data are expressed as the mean ± SD (n = 4/group). Data are analyzed by one-way ANOVA followed by Bonferroni post hoc. Asterisks indicate significances: *p < 0.05, **p < 0.01, and ***p < 0.001. CIMT: constraint-induced movement therapy, VGAT: vesicular GABA amino acid transporter, GAD65: glutamic acid decarboxylase 65, GLU: glutamate, NE: norepinephrine, DA: dopamine, ACH: acetylcholine.

5G, H). The real-time PCR measurement showed that the mRNA expression levels of VEGF and BDNF were significantly upregulated in the CIMT group compared with the Spont group. There was no apparent difference between the Sham and Spont groups (Figure 5I, J). Subsequently, we investigated cfos activity, a marker for activated neurons, to evaluate the efficacy of CIMT stimulation. The number of cfos $^{+}$NEUN^{+} cells was significantly downregulated in the Spont group in the contralesional cortex as compared to the Sham (p < 0.05) and CIMT group (p < 0.0001). However, there was no significant difference in the number of cfos^{+}NEUN^{+} cells between the CIMT and Sham groups (Figure 5K, L).

6. CIMT promoted an excitation-inhibitory signal balance of neurons by inducing neurotransmitter homeostasis in the contralesional cortex. Cellular calcium ion homeostasis was associated with synaptic plasticity by regulating neurotransmitter release.[17] The regulated proteins of neurotransmitters, such as VGAT, GAD65, and HTR2C, were assessed by Western blotting. The VGAT level was significantly upregulated in the CIMT group as compared to the Sham (p < 0.001) and Spont group (p < 0.01) (Figure 6A, B). The GAD65 expression (p < 0.05) was increased in the Spont group compared to the Sham group. However, the expression of GAD65 (p < 0.05) was significantly decreased in the CIMT group as compared to the Spont group (Figure 6C, D). The expression of HTR2C (p < 0.05) was significantly downregulated in the Spont group as compared to the Sham and CIMT group (Figure 6E, F). The number of GAD65^{+}NEUN^{+} cells (p < 0.01) also obviously increased in the ischemic and contralesional cortex in the Spont group

https://doi.org/10.1021/acsomega.4c02537
ACS Omega 2024, 9, 21612–21625

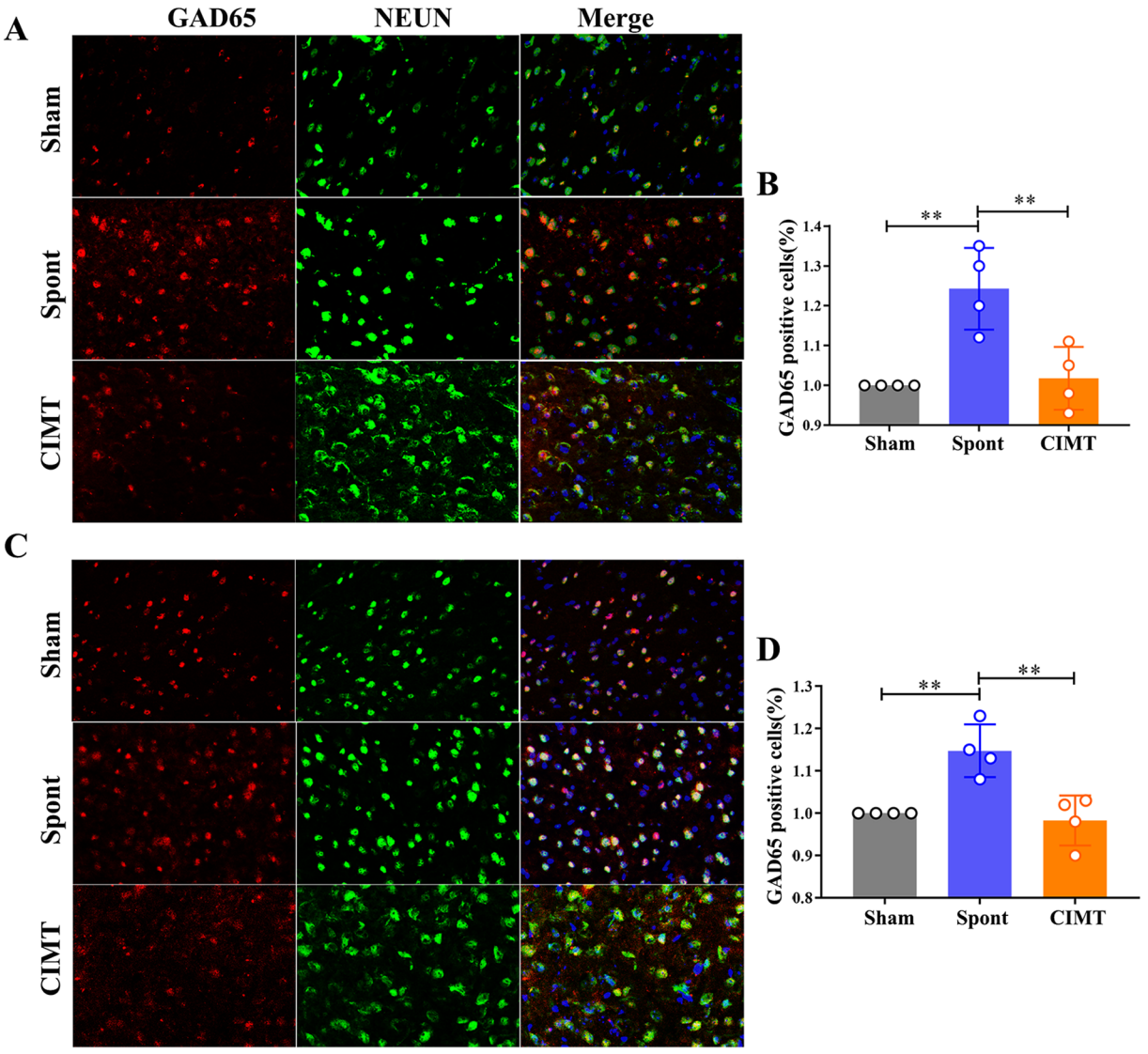

Figure 7. CIMT decreased the expression of GAD65 on the bilateral cortex. (A) The expression of GAD65 on the ischemic cortex assessed by IF; (B) Quantitative analysis showing the expression of GAD65 on the ischemic cortex; (C) The expression of GAD65 on the contralateral cortex assessed by IF; and (D) Quantitative analysis showing the expression of GAD65 on the contralateral cortex. Data are expressed as the mean ± SD (n = 4/group). Data are analyzed by one-way ANOVA followed by Tukey's multiple comparisons test. Asterisks indicate significances: *p < 0.05, **p < 0.01, and ***p < 0.001. CIMT: constraint-induced movement therapy, GAD65: glutamic acid decarboxylase 65.

compared to the Sham group. However, the number of $GAD65^{+}NEUN^{+}$ cells (p < 0.01) was significantly lower in the CIMT group than in the Spont group (Figure 7A–D).

On the 21st day after MCAO surgery, we also explored the neurotransmitter content in the unaffected cortex using HPLC. There was an apparently increased glutamate (p < 0.05, Figure 6G) and a remarkable decrease in GABA (p < 0.05, Figure 6H) in the CIMT group as compared with those in the Spont group. However, there was no significant difference in the NE, DA, and ACH levels among the Sham, Spont, and CIMT groups (p > 0.05, Figure 6I–K). Those results suggested that CIMT can increase neural activity and promote functional compensation in the contralesional cortex.

7. The Potential Mechanism of CIMT Reversed Motor Dysfunction Was Associated with the Calcium Iron Homeostasis in the Contralesional Cortex. There were 9 associated genes involved in calcium ion homeostasis that potentially exerted essential roles, including "Ccl8″, "Cxcl10″, "Cxcl9″, "Htr2c", "Npsr1", "Trpc2", "Trhr", "Pde6a", and "Vdr" (Figure 8A). Furthermore, we further assessed the mRNA levels of "Htr2c", "Npsr1", "Trpc2", and "Trhr" on the contralateral cortex among the three groups. The mRNA levels of Trpc2 (p < 0.05) and Trhr (p < 0.01) were significantly increased in the CIMT group as compared to those in the Sham group and Spont group (Figure 8B and C). Htr2c mRNA levels (p < 0.05) were significantly upregulated in the CIMT group than those in the Spont group (Figure 8D). The mRNA levels of Npsr1 in the Spont group were significantly increased compared to the Sham group (p < 0.01). Meanwhile, the mRNA levels of Npsr1 (p < 0.001) in the CIMT group were also obviously increased as compared to the Sham group (Figure 8E). There were no significant differences between the Spont and CIMT groups.

https://doi.org/10.1021/acsomega.4c02537
ACS Omega 2024, 9, 21612−21625

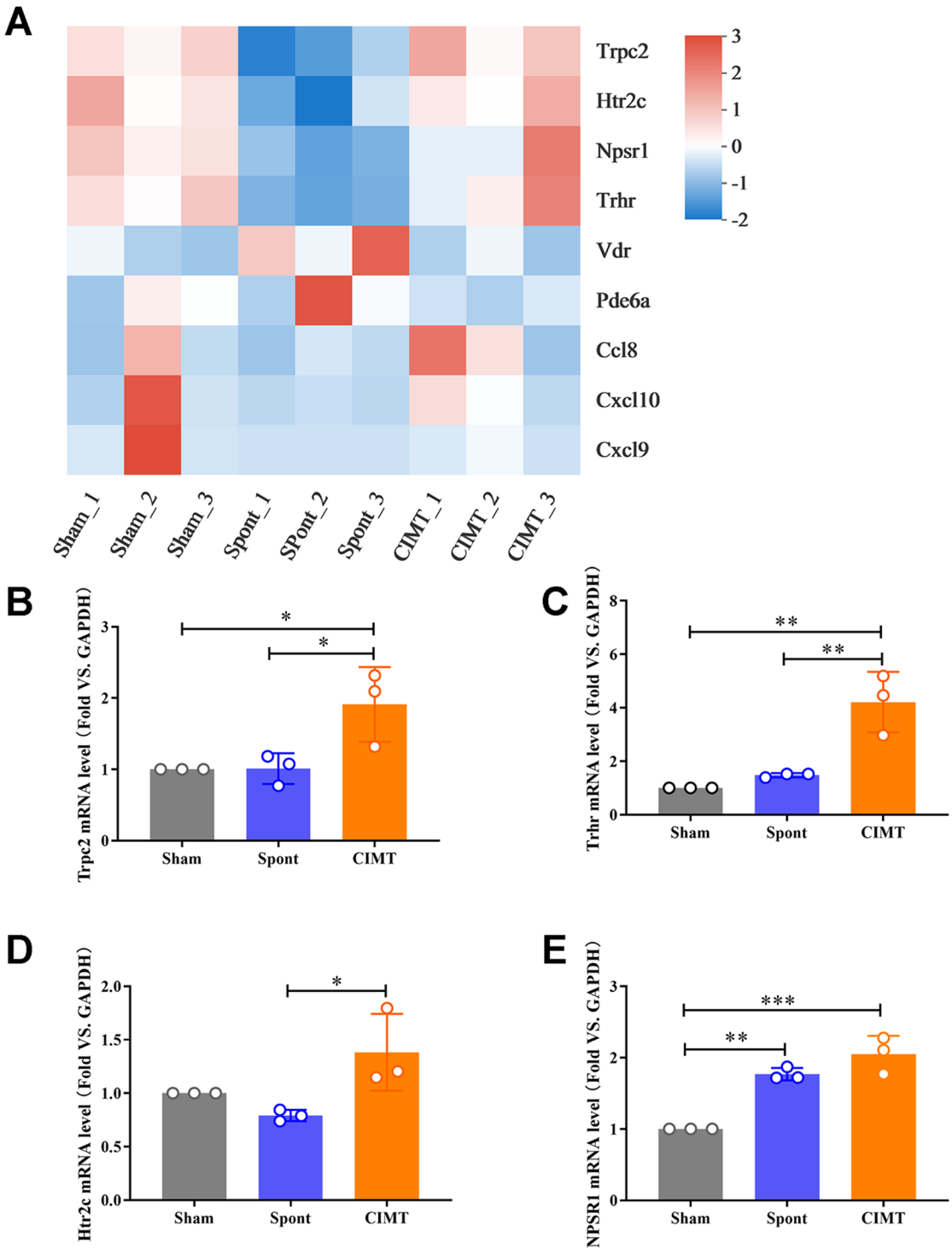

Figure 8. CIMT induced the cellular calcium ion homeostasis in the contralateral cortex after ischemic stroke. (A) The most biological process-related genes were annotated with GO terms and were involved in "calcium ion homeostasis", including Trpc2, Htr2c, NPSR1, Trhr, Vdr, Pde6a, Ccl8, Cxcl10, and Cxcl9 (n = 3). (B–E) The mRNA levels of Trpc2, Htr2c, NPSR1, and Trhr were assessed by the real-time PCR. Data are expressed as the mean ± SD (n = 3). Data are analyzed by one-way ANOVA followed by Bonferroni post hoc. Asterisks indicate significances: *p < 0.05, **p < 0.01, and ***p < 0.001. CIMT: constraint-induced movement therapy.

DISCUSSION

The present study aimed to evaluate the impact of CIMT on the synaptic plasticity of the contralateral cortex following an ischemic stroke. Our findings suggest that CIMT enhances the participation of neurons from the contralateral cortex in the forelimb-innervating network. The underlying mechanism for this enhancement may be associated with homeostatic regulation of neurotransmission.

CIMT has been developed to address upper limb impairments poststroke. It is currently the most extensively researched intervention for the rehabilitation of patients.[18]

https://doi.org/10.1021/acsomega.4c02537
ACS Omega 2024, 9, 21612−21625

However, specific mechanisms remain unidentified. In recent years, CIMT has also been widely applied in the cerebral ischemic animal model. CIMT can effectively contribute to nerve regeneration and angiogenesis at 4 weeks following stroke, and it might partially be done by inhibiting the Nogo-A/RhoA/ROCK pathway.[19] In our previous study, CIMT can noticeably improve motor function of rats in 21 days and 28 days after cerebral ischemic stroke.[20] In this study, the mNSS and Catwalk tests showed noticeable improvement in the motor function of ischemic stroke (Figure 2B−J).

A clinical study demonstrated that larger lesion volumes and increased severity in the corticospinal tract (CST), particularly in CST fibers originating from the lesioned primary motor cortex (M1), were associated with a more significant impairment of hand function. This association is crucial in determining the extent of contralateral M1 reorganization.[21] It was reported that there was a reduction in the size and volume of the ipsilesional cortical hand motor representation, along with an anterior-medial shift of the contralesional hand motor representation within the contralesional primary motor cortex.[22] The combination with cTBS over the contralesional primary motor cortex and upper limb training promoted recovery of the upper limb, reduced disability and dependence, and led to earlier discharge from the rehabilitation center in patients within 3 weeks after stroke onset.[23] In the animal study, optogenetically activated contralesional corticospinal neurons promoted axonal sprouting to the denervated hemicord after severe ischemic stroke by facilitating the formation of new functional circuits through synaptogenesis, providing a new therapeutic target.[24,25] However, the mechanism of the contralesional cortex in improving the limb's recovery remained unclear. Therefore, we used PRV retrograde nerve tracing to explore the role of the contralesional cortex in improving the affected upper limb. We found that CIMT can elicit more neuron recruitment in the M1 and S1 areas of the contralesional hemisphere than in the ipsilesional hemisphere (Figure 3). Those results indicated the critical role of the contralesional hemisphere in CIMT-induced recovery, in terms of structural reorganization.

Previous studies have found the contralesional cortex's important role in recovery after stroke,[26,27] whereas the mechanisms still need to be explored. Using transcriptome-wide RNA sequencing, we found 169 differentially expressed genes in the contralesional cortex among the Sham, Spont, and CIMT groups (Figure 4A-B). We further analyzed the biological function of differentially expressed genes using GO annotation analysis, finding that the most biological process-related genes were involved in the "gamma-aminobutyric acid signaling pathway", "regulation of gamma-aminobutyric acid secretion", and "regulation of synaptic transmission, cholinergic" (Figure 4E). The associated enriched pathway by KEGG enrichment analysis was involved in the "VEGF signaling pathway" and "Glutamatergic synapse" (Figure 4F). Our results demonstrated that synaptic plasticity exerted an essential role in the CIMT-induced functional recovery. However, these results still require further verification.

Synaptic plasticity plays a pivotal role in neural recovery following brain injury. A dynamic equilibrium that balances the synthesis and degradation of synaptic proteins is critical for preserving synaptic plasticity. Nevertheless, following an ischemic stroke, axonal termini undergo degeneration, leading to the disintegration of the synaptic structure, which is further characterized by diminished expressions of PSD-95 and SYN.[28,29] In the present study, we consistently found that CIMT significantly increased the expressions of synaptic associated proteins in the contralateral cortex, including SYN, PSD95, CREB and GAP43 (Figure 5A−H). The neurotrophic factors brain-derived neurotrophic factor (BDNF) and vascular endothelial growth factor (VEGF) also showed significant upregulation in the contralateral cortex after CIMT (Figure 5I, J). In this study, we utilize cfos as an indirect indicator of neuronal activity. We found that CIMT notably augmented the expression of synaptic activity in the contralateral cortex (Figure 5K, L). Those results suggested that CIMT can increase synaptic plasticity in the contralateral cortex.

We also detected the neurotransmitters associated with protein levels, including VGAT, GAD65, and HTR2C. VGAT is a vesicular GABA transporter whose primary function is transporting GABA to synaptic vesicles to regulate GABA signaling.[30] GAD65 or GAD67 are crucial enzymes for synthesizing GABA in the somatic cells.[31] Serotonin (5-HT) receptors, especially 5-HT2C receptors (HTR2C), appear to contribute to the gradual restoration of sustained the constant inward current of motor neurons, which is crucial for motor function recovery.[32] In this study, CIMT significantly increased the expression of VGAT and HTR2C, whereas CIMT decreased the GAD65 level (Figure 6A−F).

Furthermore, we explored the regulation of changes in transmitter release by using HPLC. Notably, the Glutamate level significantly increased and the GABA level markedly decreased in the contralesional cortex (Figure 6G, H). It is further suggested that CIMT regulates neurotransmitter homeostasis in the healthy cortex to promote an excitation-inhibitory signal balance of neurons. In a previous study, the neurotransmitter level might be related to the size and location of the ischemic area. When a severe ischemic cerebral infarction occurs, the contralesional cortex will be activated to compensate for the impaired brain tissue.[33] Thus, those results demonstrated that CIMT can improve synaptic plasticity by increasing neuronal excitability and facilitating glutamate release.

It has been reported that the concentration of calcium ions can regulate transmitter release in presynaptic terminals and long-term plastic changes of synaptic efficiency.[34] As shown by Silva M et al., the latest review discussed that calcium can modify synaptic strength by regulating a final, rapid vesicle maturation step before transmitter release.[35] Notably, the biological function of differentially expressed genes using GO annotation analysis also found that the most biological process-related genes were involved in "cellular calcium ion homeostasis", indicating the vital role of cellular calcium ion homeostasis in CIMT to improve motor function. We further assessed the mRNA levels of associated genes involved in calcium ion homeostasis, including "Htr2c", "Npsr1", "Trpc2", and "Trhr" (Figure 8A). CIMT can regulate the mRNA levels of those genes on the contralateral cortex, which might be a key mechanism of synaptic plasticity changes (Figure 8B−E). This result indicated the important role of cellular calcium ion homeostasis in CIMT-induced synaptic plasticity.

Together, our results reveal important implications of CIMT-mediated mechanisms for stroke recovery. At the behavior and molecular level, we demonstrated that CIMT is involved in mechanisms of neuronal plasticity that contribute to functional recovery following ischemic stroke. By PRV retrograde nerve tracing, we found that CIMT can recruit

https://doi.org/10.1021/acsomega.4c02537
ACS Omega 2024, 9, 21612−21625

neurons of the contralesional hemisphere into the innervating network of the affected upper limb, indicating the critical role of the contralesional hemisphere in CIMT-induced structural reorganization. The associated mechanism might be involved in CIMT-increased neuronal excitability by regulating neurotransmitter levels and cellular calcium iron homeostasis. Based on our findings, it will be possible to develop specific rehabilitation strategies targeting CIMT-mediated mechanisms in the brain after an ischemic stroke.

Materials and Methods. *Animals.* Male C57BL/6J mice were 8−12 weeks old from Charles River (Beijing, China). All mice were housed in a temperature-controlled facility under a standard 12 h light: dark cycle with food and water ad libitum. The Fudan University Animal Care and Use Committee authorized all experimental procedures (approval no. 2022JS Huashan Hospital-082) on February 25, 2022. All experiments were performed in accordance with the National Institutes of Health's Guide for the Care and Use of Laboratory Animals.[36] The experimental methods and schedules are presented in Figure 1E.

MCAO Model. The MCAO model was established as previously described, following anesthesia with 1% pentobarbital sodium with 1% pentobarbital sodium (1 mg/mL, intraperitoneally).[37] Briefly, the left common carotid artery (CCA), internal carotid artery (ICA) and external carotid artery (ECA) were exposed and isolated, followed by the distal ECA cut with a small slit. The middle cerebral artery was occluded for 60 min by a silicon-coated monofilament (Guangzhou Jialing Co., Ltd.) that was inserted into the ICA from the slit of the ECA. After the monofilament was pulled out, the surgical incision was disinfected and sutured. In the surgical period, the body temperature was maintained at 35 °C using a heating pad. The blood flow was monitored using laser Doppler anemometry (RWD Life Science, Shenzhen, China) pre-MCAO, during MCAO, and 5 min after reperfusion. Mice with a decline in regional cerebral blood flow (rCBF) ≥ 70% of pre-MCAO baseline levels were considered a successful occlusion. A modified neurological severity score (mNSS) was used to evaluate the neurological deficit 24 h after surgery. Animals were randomized to the Spont group and the CIMT group if the mNSS score ≥6 points. In the sham group, mice underwent the same operation but did not insert a monofilament.

Constraint-Induced Movement Therapy (CIMT). Mice from the CIMT group underwent CIMT during 7−14 days after MCAO surgery. CIMT was performed by restricting the unaffected upper limb of ischemic mice and positioning it in a naturally retracted position by a plaster. Subsequently, mice were forced to use the affected forelimb with food and water. In the Spont group, mice were tied to the plaster without restriction of the unaffected forelimb.

2,3,5-Triphenyltetrazolium Chloride (TTC) Staining. TTC staining was used to measure infarct volume after MCAO/R. Briefly, brains were cut to 2 mm-thick coronal blocks and were immersed in 2% TTC solution at 37∘C for 30 min after 72h of reperfusion. The infarct region area and the total area of each brain slice were quantified by using ImageJ software (NIH, USA). The infarct volume (%) = (infarct area/total brain area) × 100%.

Quantitative Real-Time PCR. Total RNA was extracted from the contralateral cortex using TRIzol Reagent (Invitrogen, United States). Complementary DNA synthesis was performed using Prime Script RT Master Mix Invitrogen). Real-time PCR was performed using a TB Green Kit (TB Green Premix Ex Taq TaKaRa, Japan). RNA sequences were purchased from BioTNT Biotechnologies (China) as follows:

Trhr (Forward: 5′-AATGCCACCAACAGATGCTT-CAAC-3′;
Reverse: 5′-TGGAAAGGGCTGGAGAGAAATGAG−3′);
NPSR1(Forward: 5′-CCGCCTTGAACAGTGCCAT-TAAC-3′;
Reverse: 5′-CATCTCGTGTCTCTCGCTTCTCTC-3′);
TRPC2 (Forward: 5′-TCACGAATCGCTGGGCA-CAC-3′;
Reverse: 5′-CACAGAGGAAGGCAGTCAGGATG-3′);
5HTR2C (Forward: 5′-GGTCCTTCGTGGCATTCTTCATCC-3′;
Reverse: 5′ -TACGCAGTTCCTCCTCGGTGTG-3′);
VEGF (Forward: 5′-GGGCTCTTCTCGCTCCGTAG-TAG-3′;
Reverse: 5′−CCCTCTCCTCTTCCTTCTCTTCCTC-3′);
BDNF (Forward: 5′ -CGACGACATCACTGGCTGA-CAC-3′;
Reverse: 5′ -GAGGCTCCAAAGGCACTTGACTG-3′);
GAPDH (Forward: 5′-AGAAGGTGGTGAAGCAGG-CATC-3′;
Reverse: 5′ -CGAAGGTGGAAGAGTGGGAGTTG-3′).

We used the 2D CT method to calculate relative mRNA expression normalized to GAPDH.

Retrograde Tracing by PRV. On the 21st day after MCAO, as previously described,[38] the right brachial plexus was exposed and severed. The proximal end of the severed brachial plexus was dipped into the PRV so that all mice infected the PRV (PRV-CAG-EGFP, BrainVTA Co., Ltd., Wuhan, China) for 20 min. Four to 6 days after infection, the brain tissues were isolated by dehydration in a 30% sucrose solution and sliced into 30-um thick sections. DAPI (Southern Biotech, Birmingham, AL, USA) was used to mark the cell nuclei. The immunofluorescence was observed with a confocal microscope and was analyzed with ImageJ software.

Preparation of Tissue and Western Blotting. Mice in the two groups were sacrificed 21 days after MCAO surgery. Total proteins were extracted from the contralesional cortex. A BCA kit (solarbio, Beijing) measured the protein concentration. Equal amounts of proteins from each sample were loaded by 12% SDS-PAGE at 100 V for 90 min and then transferred to the PVDF membranes(Roche, Switzerland) at 80 V for 60 min. Subsequently, the PVDF membranes were blocked in 5% defatted milk powder for 1 h at 37 °C. We then prepared the primary antibodies: anti-PSD 95 (1:1000, cell signal technology), anti-GAP43 (1:2000, abmart), anti-SYN (1:500, proteintech), vesicular GABA amino acid transporter(VGAT) (1:1000, proteintech), Glutamic acid decarboxylase 65 (GAD65, 1:3000, proteintech), Tubulin (1:5000; abmart), and HTR2C (1:1000; abmart). After incubating with the primary antibodies at 4 °C and washing with PBST, membranes were treated with horseradish peroxidase-conjugated secondary antibodies (1:5000) for 1 h at room temperature. Finally, membranes were immunodetected by enhanced ECL chromogenic substrates and measured by

https://doi.org/10.1021/acsomega.4c02537
ACS Omega 2024, 9, 21612−21625

ImageJ software. The protein levels were normalized to Tubulin or GAPDH (1:5000; Proteintech).

Catwalk Test. The catwalk test was used to assess the gait parameters in ischemic mice. Before the test, a 1.5m-long glass track was cleaned with 75% ethyl alcohol. Subsequently, the mouse was individually placed on the glass track and was allowed to pass freely. A camera positioned below the photo was used to record each paw. The 60% maximum speed variation and the run duration between 0.50 and 5.00 s were defined as successful runs. Three compliant runs were required per trial in each mouse. The paw-related parameters were calculated using the Catwalk XT system (Noldus, The Netherlands, Wageningen). After the experiments, all mice were classified into four limbs and statistically analyzed.

Preparation of Tissue and Immunofluorescence. After the behavior test, mice were anesthetized with 1% pentobarbital sodium, followed by perfusion with 0.9% normal saline, and fixation with 4% paraformaldehyde at 4 °C for 24 h. Before immunofluorescence, brains were dehydrated in a 30% sucrose solution and then sliced into sections at 20 um thick by a freezing microtome. Briefly, brain slices were incubated with 0.3% Triton for 10 min, followed by blocking with 5% bovine serum albumin (BSA). Primary antibodies, GAD65 (1:300, proteintech), cfos (1:400, SYSY), and NEUN (1:400, Novus), were prepared for immunofluorescence. Then, the brain slices were incubated with primary antibodies at 4 °C overnight. After being washed with 0.01 M PBS, secondary antibodies conjugated to 488 or 594 (Thermo Fisher Scientific) were used to incubate for 1.5 h. DAPI (Southern Biotech, Birmingham, AL, USA) was used to mark the cell nuclei. The immunofluorescence was observed with a confocal microscope, and the fluorescence intensity was analyzed by using ImageJ software.

RNA Sequencing and Differentially Expressed Gene Analysis. At 21 days after the ischemic stroke, mice were sacrificed and the contralesional cortex was dissected on ice. RNA was isolated using the TRIzol reagent (Invitrogen, Carlsbad, CA, USA). A TruSeq Stranded mRNA LT Sample Prep Kit (Illumina, San Diego, CA, USA) generated RNA sequencing libraries according to the manufacturer's instructions. After that, the libraries were sequenced by an Illumina Hiseq X10. At last, the data were analyzed on a free online platform, Majorbio Cloud Platform (www.majorbio.com). Data analysis statisticians were blinded to the experimental group information. P value <0.05 and fold-change >2.0 was set as the threshold for significantly differential expression.

High-Performance Liquid Chromatography (HPLC). The contralesional cortex was collected from the decapitated mice 3 weeks after MCAO surgery. The sample was weighed on a balance pan, and 0.4 N perchloric acid solution was added according to the weight of the sample. The solution was ultrasonically homogenized five times for 10−20 s. After that, the supernatant was taken out after 10,000 rpm centrifugation for 10 min. The levels of GAMMA-amino butyric acid (GABA), glutamate (GLU), dopamine (DA), acetylcholine (ACH), and norepinephrine (NE) were measured by using HPLC (Agilent Technologies, Santa Clara, CA, USA). The detailed experiment method is as described previously.[20] The data were analyzed by ChemStation (Agilent Technologies).

Statistical Analysis. GraphPad Prism 8 was used to perform statistical analysis. Data are analyzed by one-way ANOVA followed by Bonferroni post hoc or Tukey's multiple comparisons test. Survival percentages were assessed using survival analysis and a log-rank test. Data are expressed as mean ± SD. The level of statistical significance was set at $*p < 0.05$, $**p < 0.01$, $***p < 0.001$.

AUTHOR INFORMATION

Corresponding Authors

Zhanzhuang Tian − *Department of Integrative Medicine and Neurobiology, School of Basic Medical Sciences, State Key Laboratory of Medical Neurobiology and MOE Frontiers Center for Brain Science, Institutes of Brain Science, Institute of Acupuncture Research, Academy of Integrative Medicine, Shanghai Key Laboratory for Acupuncture Mechanism and Acupoint Function, Shanghai Medical College, Fudan University, Shanghai 200433, China*; Email: tianvv@shmu.edu.cn

Yulong Bai − *Department of Rehabilitation Medicine, Huashan Hospital, Fudan University, Shanghai 200040, P.R. China; National Center for Neurological Disorders, Huashan Hospital, Fudan University, Shanghai 200040, P.R. China*; orcid.org/0000-0003-0461-1506; Email: dr_baiyl@fudan.edu.cn

Authors

Anjing Zhang − *Department of Rehabilitation Medicine, Huashan Hospital, Fudan University, Shanghai 200040, P.R. China; Department of Neurological Rehabilitation Medicine, The First Rehabilitation Hospital of Shanghai, Shanghai 200093, P.R. China*

Ying Xing − *Department of Rehabilitation Medicine, Huashan Hospital, Fudan University, Shanghai 200040, P.R. China*

Jiayuan Zheng − *Department of Integrative Medicine and Neurobiology, School of Basic Medical Sciences, State Key Laboratory of Medical Neurobiology and MOE Frontiers Center for Brain Science, Institutes of Brain Science, Institute of Acupuncture Research, Academy of Integrative Medicine, Shanghai Key Laboratory for Acupuncture Mechanism and Acupoint Function, Shanghai Medical College, Fudan University, Shanghai 200433, China*

Congqin Li − *Department of Rehabilitation Medicine, Huashan Hospital, Fudan University, Shanghai 200040, P.R. China*

Yan Hua − *Department of Rehabilitation Medicine, Huashan Hospital, Fudan University, Shanghai 200040, P.R. China*

Jian Hu − *Department of Rehabilitation Medicine, Huashan Hospital, Fudan University, Shanghai 200040, P.R. China*

Complete contact information is available at: https://pubs.acs.org/10.1021/acsomega.4c02537

Author Contributions

†Co-first authors: Anjing Zhang and Ying Xing contributed equally to this work. Anjing Zhang and Yulong Bai had the initial idea for this article; Anjing Zhang and Ying Xing drafted the manuscript; Jiayuan Zheng and Ying Xing prepared all the figures; Anjing Zhang and Jiayuan Zheng analyzed data; Yan Hua and Ying Xing prepared the animal experiments; Jiayuan Zheng, Congqin Li, and Jian Hu performed the molecular experiments; Zhanzhuang Tian assisted with experimental procedures and provided access to the experimental facilities. Anjing Zhang, Jiayuan Zheng, Zhanzhuang Tian, and Yulong Bai critically revised the manuscript; Yulong Bai and Zhanzhuang Tian approved the final version of the manuscript, and Yulong Bai provided the funds.

https://doi.org/10.1021/acsomega.4c02537
ACS Omega 2024, 9, 21612−21625

Funding

This study was funded by the National Natural Science Foundation of China (grant number 82072540).

Notes

The authors declare no competing financial interest.

REFERENCES

(1) Tater, P.; Pandey, S. Post-stroke Movement Disorders: Clinical Spectrum, Pathogenesis, and Management. *Neurol India* **2021**, *69* (2), 272−283.

(2) Meng, L.; Liang, Q.; Yuan, J.; Li, S.; Ge, Y.; Yang, J.; Tsang, R. C. C.; Wei, Q. Vestibular rehabilitation therapy on balance and gait in patients after stroke: a systematic review and meta-analysis. *BMC Med.* **2023**, *21* (1), 322.

(3) Wang, D.; Xiang, J.; He, Y.; Yuan, M.; Dong, L.; Ye, Z.; Mao, W. The Mechanism and Clinical Application of Constraint-Induced Movement Therapy in Stroke Rehabilitation. *Front Behav Neurosci* **2022**, *16*, 828599.

(4) Li, C.; Hu, J.; Xing, Y.; Han, J.; Zhang, A.; Zhang, Y.; Hua, Y.; Tian, Z.; Bai, Y. Constraint-induced movement therapy alleviates motor impairment by inhibiting the accumulation of neutrophil extracellular traps in ischemic cortex. *Neurobiol Dis* **2023**, *179*, 106064.

(5) Reddy, R. S.; Gular, K.; Dixit, S.; Kandakurti, P. K.; Tedla, J. S.; Gautam, A. P.; Sangadala, D. R. Impact of Constraint-Induced Movement Therapy (CIMT) on Functional Ambulation in Stroke Patients-A Systematic Review and Meta-Analysis. *Int. J. Environ. Res. Public Health* **2022**, *19* (19), 12809.

(6) Dabrowski, J.; Czajka, A.; Zielinska-Turek, J.; Jaroszynski, J.; Furtak-Niczyporuk, M.; Mela, A.; Poniatowski, L. A.; Drop, B.; Dorobek, M.; Barcikowska-Kotowicz, M.; Ziemba, A. Brain Functional Reserve in the Context of Neuroplasticity after Stroke. *Neural Plast* **2019**, *2019*, 9708905.

(7) Xing, Y.; Bai, Y. A Review of Exercise-Induced Neuroplasticity in Ischemic Stroke: Pathology and Mechanisms. *Mol. Neurobiol* **2020**, *57* (10), 4218−4231.

(8) Wang, Q.; Wills, M.; Li, F.; Geng, X.; Ding, Y. Remote ischemic conditioning with exercise (RICE) promotes functional rehabilitation following ischemic stroke. *Neurol Res.* **2021**, *43* (11), 874−883.

(9) Liu, X. H.; Bi, H. Y.; Cao, J.; Ren, S.; Yue, S. W. Early constraint-induced movement therapy affects behavior and neuronal plasticity in ischemia-injured rat brains. *Neural Regen Res.* **2019**, *14* (5), 775−782.

(10) Okabe, N.; Himi, N.; Maruyama-Nakamura, E.; Hayashi, N.; Narita, K.; Miyamoto, O. Rehabilitative skilled forelimb training enhances axonal remodeling in the corticospinal pathway but not the brainstem-spinal pathways after photothrombotic stroke in the primary motor cortex. *PLoS One* **2017**, *12* (11), No. e0187413.

(11) Wang, Q.; Kohls, W.; Wills, M.; Li, F.; Pang, Q.; Geng, X.; Ding, Y. A novel stroke rehabilitation strategy and underlying stress granule regulations through inhibition of NLRP3 inflammasome activation. *CNS Neurosci Ther* **2024**, *30* (1), No. e14405.

(12) Mizutani, K.; Sonoda, S.; Yamada, K.; Beppu, H.; Shimpo, K. Alteration of protein expression profile following voluntary exercise in the perilesional cortex of rats with focal cerebral infarction. *Brain Res.* **2011**, *1416*, 61−8.

(13) Calautti, C.; Jones, P. S.; Naccarato, M.; Sharma, N.; Day, D. J.; Bullmore, E. T.; Warburton, E. A.; Baron, J. C. The relationship between motor deficit and primary motor cortex hemispheric activation balance after stroke: longitudinal fMRI study. *J. Neurol Neurosurg Psychiatry* **2010**, *81* (7), 788−92.

(14) Liu, G.; Dang, C.; Chen, X.; Xing, S.; Dani, K.; Xie, C.; Peng, K.; Zhang, J.; Li, J.; Zhang, J.; Chen, L.; Pei, Z.; Zeng, J. Structural remodeling of white matter in the contralesional hemisphere is correlated with early motor recovery in patients with subcortical infarction. *Restor Neurol Neurosci* **2015**, *33* (3), 309−19.

(15) Okabe, N.; Himi, N.; Nakamura-Maruyama, E.; Hayashi, N.; Sakamoto, I.; Narita, K.; Hasegawa, T.; Miyamoto, O. Constraint-induced movement therapy improves efficacy of task-specific training after severe cortical stroke depending on the ipsilesional corticospinal projections. *Exp. Neurol.* **2018**, *305*, 108−120.

(16) Liu, P.; Li, C.; Zhang, B.; Zhang, Z.; Gao, B.; Liu, Y.; Wang, Y.; Hua, Y.; Hu, J.; Qiu, X.; Bai, Y. Constraint induced movement therapy promotes contralesional-oriented structural and bihemispheric functional neuroplasticity after stroke. *Brain Res. Bull.* **2019**, *150*, 201−206.

(17) Padamsey, Z.; Foster, W. J.; Emptage, N. J. Intracellular Ca(2+) Release and Synaptic Plasticity: A Tale of Many Stores. *Neuroscientist* **2019**, *25* (3), 208−226.

(18) Kwakkel, G.; Veerbeek, J. M.; van Wegen, E. E.; Wolf, S. L. Constraint-induced movement therapy after stroke. *Lancet Neurol* **2015**, *14* (2), 224−34.

(19) Zhai, Z. Y.; Feng, J. Constraint-induced movement therapy enhances angiogenesis and neurogenesis after cerebral ischemia/reperfusion. *Neural Regen Res.* **2019**, *14* (10), 1743−1754.

(20) Gao, B. Y.; Xu, D. S.; Liu, P. L.; Li, C.; Du, L.; Hua, Y.; Hu, J.; Hou, J. Y.; Bai, Y. L. Modified constraint-induced movement therapy alters synaptic plasticity of rat contralateral hippocampus following middle cerebral artery occlusion. *Neural Regen Res.* **2020**, *15* (6), 1045−1057.

(21) Buetefisch, C. M.; Haut, M. W.; Revill, K. P.; Shaeffer, S.; Edwards, L.; Barany, D. A.; Belagaje, S. R.; Nahab, F.; Shenvi, N.; Easley, K. Stroke Lesion Volume and Injury to Motor Cortex Output Determines Extent of Contralesional Motor Cortex Reorganization. *Neurorehabil Neural Repair* **2023**, *37* (2−3), 119−130.

(22) Veldema, J.; Bosl, K.; Nowak, D. A. Motor Recovery of the Affected Hand in Subacute Stroke Correlates with Changes of Contralesional Cortical Hand Motor Representation. *Neural Plast* **2017**, *2017*, 6171903.

(23) Vink, J. J. T.; van Lieshout, E. C. C.; Otte, W. M.; van Eijk, R. P. A.; Kouwenhoven, M.; Neggers, S. F. W.; van der Worp, H. B.; Visser-Meily, J. M. A.; Dijkhuizen, R. M. Continuous Theta-Burst Stimulation of the Contralesional Primary Motor Cortex for Promotion of Upper Limb Recovery After Stroke: A Randomized Controlled Trial. *Stroke* **2023**, *54* (8), 1962−1971.

(24) Wahl, A. S.; Buchler, U.; Brandli, A.; Brattoli, B.; Musall, S.; Kasper, H.; Ineichen, B. V.; Helmchen, F.; Ommer, B.; Schwab, M. E. Optogenetically stimulating intact rat corticospinal tract post-stroke restores motor control through regionalized functional circuit formation. *Nat. Commun.* **2017**, *8* (1), 1187.

(25) Yang, Y.; Chen, X.; Yang, C.; Liu, M.; Huang, Q.; Yang, L.; Wang, Y.; Feng, H.; Gao, Z.; Chen, T. Chemogenetic stimulation of intact corticospinal tract during rehabilitative training promotes circuit rewiring and functional recovery after stroke. *Exp. Neurol.* **2024**, *371*, 114603.

(26) Wrobel, P. P.; Guder, S.; Feldheim, J. F.; Graterol Perez, J. A.; Frey, B. M.; Choe, C. U.; Bonstrup, M.; Cheng, B.; Rathi, Y.; Pasternak, O.; et al. Altered microstructure of the contralesional ventral premotor cortex and motor output after stroke. *Brain Commun.* **2023**, *5* (3), fcad160.

(27) McPherson, J. G.; Chen, A.; Ellis, M. D.; Yao, J.; Heckman, C. J.; Dewald, J. P. A. Progressive recruitment of contralesional cortico-reticulospinal pathways drives motor impairment post stroke. *J. Physiol* **2018**, *596* (7), 1211−1225.

(28) Yepes, M. Urokinase-type plasminogen activator is a modulator of synaptic plasticity in the central nervous system: implications for neurorepair in the ischemic brain. *Neural Regen Res.* **2020**, *15* (4), 620−624.

(29) Li, K. X.; Lu, M.; Cui, M. X.; Wang, X. M.; Zheng, Y. Astrocyte-neuron communication mediated by the Notch signaling pathway: focusing on glutamate transport and synaptic plasticity. *Neural Regen Res.* **2023**, *18* (10), 2285−2290.

(30) Lin, T. W.; Tan, Z.; Barik, A.; Yin, D. M.; Brudvik, E.; Wang, H.; Xiong, W. C.; Mei, L. Regulation of Synapse Development by Vgat Deletion from ErbB4-Positive Interneurons. *J. Neurosci.* **2018**, *38* (10), 2533−2550.

https://doi.org/10.1021/acsomega.4c02537
ACS Omega 2024, 9, 21612−21625

(31) Kajita, Y.; Mushiake, H. Heterogeneous GAD65 Expression in Subtypes of GABAergic Neurons Across Layers of the Cerebral Cortex and Hippocampus. *Front Behav Neurosci* **2021**, *15*, 750869.
(32) Talifu, Z.; Qin, C.; Xin, Z.; Chen, Y.; Liu, J.; Dangol, S.; Ma, X.; Gong, H.; Pei, Z.; Yu, Y.; Li, J.; Du, L. The Overexpression of Insulin-Like Growth Factor-1 and Neurotrophin-3 Promote Functional Recovery and Alleviate Spasticity After Spinal Cord Injury. *Front Neurosci* **2022**, *16*, 863793.
(33) Di Pino, G.; Pellegrino, G.; Assenza, G.; Capone, F.; Ferreri, F.; Formica, D.; Ranieri, F.; Tombini, M.; Ziemann, U.; Rothwell, J. C.; Di Lazzaro, V. Modulation of brain plasticity in stroke: a novel model for neurorehabilitation. *Nat. Rev. Neurol* **2014**, *10* (10), 597−608.
(34) Lopes, J. P.; Cunha, R. A. What is the extracellular calcium concentration within brain synapses?: An Editorial for 'Ionized calcium in human cerebrospinal fluid and its influence on intrinsic and synaptic excitability of hippocampal pyramidal neurons in the rat' on page 452. *J. Neurochem* **2019**, *149* (4), 435−437.
(35) Silva, M.; Tran, V.; Marty, A. Calcium-dependent docking of synaptic vesicles. *Trends Neurosci* **2021**, *44* (7), 579−592.
(36) In *Guide for the Care and Use of Laboratory Animals*, 8th ed.; The National Academies Press: Washington (DC), 2011.
(37) Xing, Y.; Zhang, A.; Li, C.; Han, J.; Wang, J.; Luo, L.; Chang, X.; Tian, Z.; Bai, Y. Corticostriatal Projections Relying on GABA Levels Mediate Exercise-Induced Functional Recovery in Cerebral Ischemic Mice. *Mol. Neurobiol* **2023**, *60* (4), 1836−1853.
(38) Wang, F.; Shen, J.; Jiang, S.; Qiu, Y.; Ye, X.; Wang, C.; Liang, C.; Xu, W. The Recognition of the Distribution Features of Corticospinal Neurons by a Retrograde Trans-synaptic Tracing to Elucidate the Clinical Application of Contralateral Middle Trunk Transfer. *Neuroscience* **2020**, *424*, 86−101.

https://doi.org/10.1021/acsomega.4c02537
ACS Omega 2024, 9, 21612−21625